Electronic Supplementary Material (ESI) for ChemComm.

# Supporting Information

## Phosphate Ion Functionalized CoP Nanowire Arrays for Efficient Alkaline Hydrogen Evolution

*Dongdong Zhu*, Liang Wang, Man Qiao, Jinlong Liu**

D. D. Zhu, M. Qiao
School of Chemistry and Materials Science, Nanjing University of Information Science and Technology, Nanjing, 210044, China.
E-mail: dd.zhu@nuist.edu.cn

L. Wang
Institute for Superconducting and Electronic Materials (ISEM), University of Wollongong, Wollongong, NSW 2525, Australia

J. L. Liu
Department of Engineering, University of Cambridge, Cambridge, CB3 0FA, United Kingdom.
Email: jl2075@cam.ac.uk

# 1. Experimental Section

## 1.1 Synthesis of Pi-CoP nanowire arrays on Ti foil

The Co-based precursor was firstly grown on the Ti foil by a hydrothermal method. In detail, 2.5 mmol $Co(NO_3)_2 \cdot 6H_2O$, 5.0 mmol $NH_4F$, and 12.5 mmol $CO(NH_2)_2$ were dissolved in 35 mL deionized water under magnetic stirring, and transferred to a Teflon-lined stainless steel autoclave (50 mL). Then a piece of clean Ti foil (2.0 cm×4.0 cm) was immersed into the reaction solution. Afterwards, the autoclave was heated at 120°C for 5 h, and then cooled down to room temperature. After the reaction, the obtained Co-based precursor was washed with deionized water and ethanol several times and dried.

Then Pi-CoP was fabricated by low-temperature phosphorization of Co-based precursor in the presence of $NaH_2PO_2 \cdot H_2O$. In detail, the obtained Co-based precursor sample and $NaH_2PO_2 \cdot H_2O$ (1.1 g) were put in porcelain boats at two detached positions with $NaH_2PO_2 \cdot H_2O$ at the upstream side of the furnace. Then under the Ar atmosphere, the furnace was elevated to 300 °C at a ramping rate of 2 °C $min^{-1}$ and held at this temperature for 2 h, and then cooled to ambient temperature at a ramping rate of 10 °C $min^{-1}$ to obtain Pi-CoP nanowire arrays. Caution!!! Since the in-situ generated $PH_3$ from the decomposition of $NaH_2PO_2 \cdot H_2O$ is extremely toxic, the post-treatment of tail gas by $CuSO_4$ solution to absorb excessive $PH_3$ is highly essential. For comparison, directly annealing Co-based precursor at 350 °C for 4 h in the air resulted in the fabrication of $Co_3O_4$ nanowire arrays.

## 1.2 Characterizations

The morphology of the samples was characterized by field emission scanning electron microscopy (FESEM, QUANTA 450) equipped with an energy dispersive spectrometer (EDS), transmission electron microscopy (TEM, Tecnai G2 Spirit, which operates at an accelerating voltage of 200 KV) and scanning transmission electron microscopy (STEM, JEOL JEM-ARM200F, which operates at an accelerating voltage of 80 KV) equipped with EDS. The powder X-ray diffractometer (XRD) data were collected using a Rigaku MiniFlex 600 with Cu Kα radiation at a scan rate of 1° $min^{-1}$. XPS measurements were carried out on an ESCALab250 using Al Kα radiation. Fourier transform infrared (FTIR) spectroscopy was recorded on a Nicolet 6700 spectrometer.

## 1.3 Electrochemical Measurements

Electrochemical tests were carried out on a workstation (CHI 760D Instruments, Inc., USA) by using a standard three-electrode glass cell (Pine Research Instruments, USA). Ag/AgCl (4 M KCl) electrode and carbon rod were used as the reference and counter electrodes, respectively, while 1.0 M KOH aqueous solution was used as the electrolyte. 1cm×1cm Pi-

CoP/Ti, $Co_3O_4$/Ti, Commercial Pt-C/Ti and bare Ti foils were investigated as the working electrodes. The reversible hydrogen electrode (RHE) potentials were obtained by the following equation: $E(RHE) = E(Ag/AgCl) + 0.205 + 0.059 \times pH$. A flow of $N_2$ (ultra-high-grade purity, Airgas) was maintained in the electrolyte during the test. Before data collection, the working electrodes were scanned by cyclic voltammetry (CV) plots until the signals were stabilized. The linear sweep voltammetry (LSV) curves were recorded with a scan rate of 1.0 mV $s^{-1}$. The obtained current densities were normalized to the geometrical surface area. Electrochemical impedance spectroscopy (EIS) was measured in the frequency range from 0.1 Hz to 100 kHz with an amplitude of 5 mV. IR compensation of LSV curves was performed using the solution resistance estimated from EIS results. The electrode durability was tested by the galvanostatic method, which was conducted at 10 mA $cm^{-2}$ for 20 hours. All the electrochemical measurements were carried out at ambient temperature.

## 2. Supplementary Figures and Tables

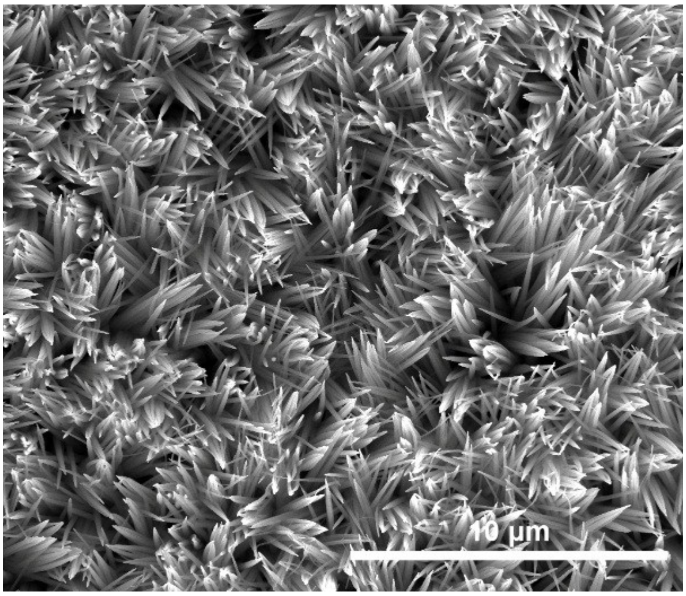

Figure S1. SEM image of Co-based precursor grown on Ti foil.

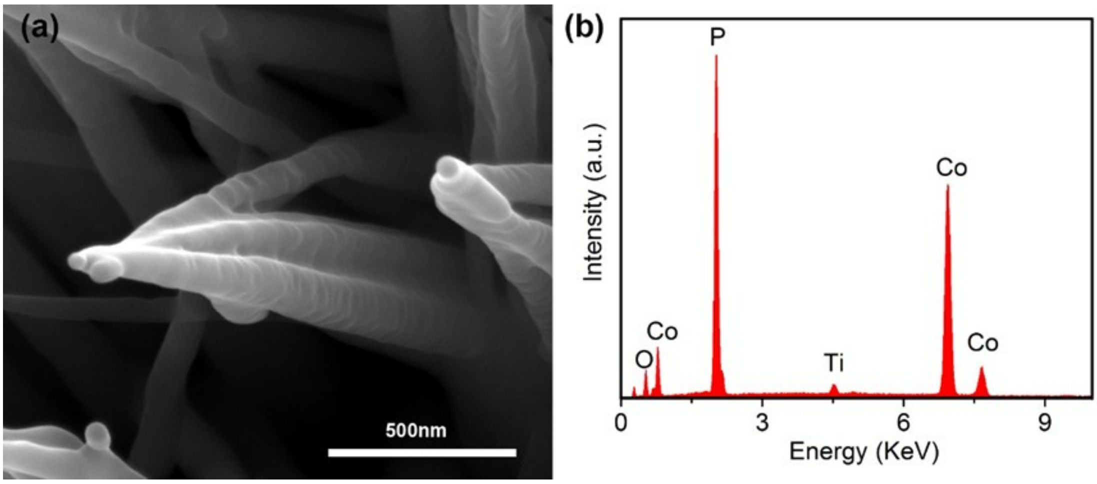

Figure S2. (a) SEM image of Pi-CoP. (b) EDS spectrum of Pi-CoP.

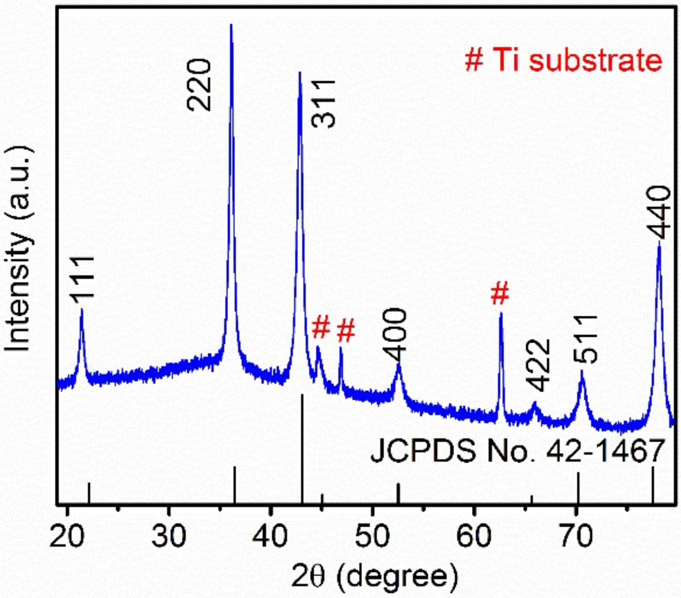

Figure S3. XRD Pattern of $Co_3O_4$.

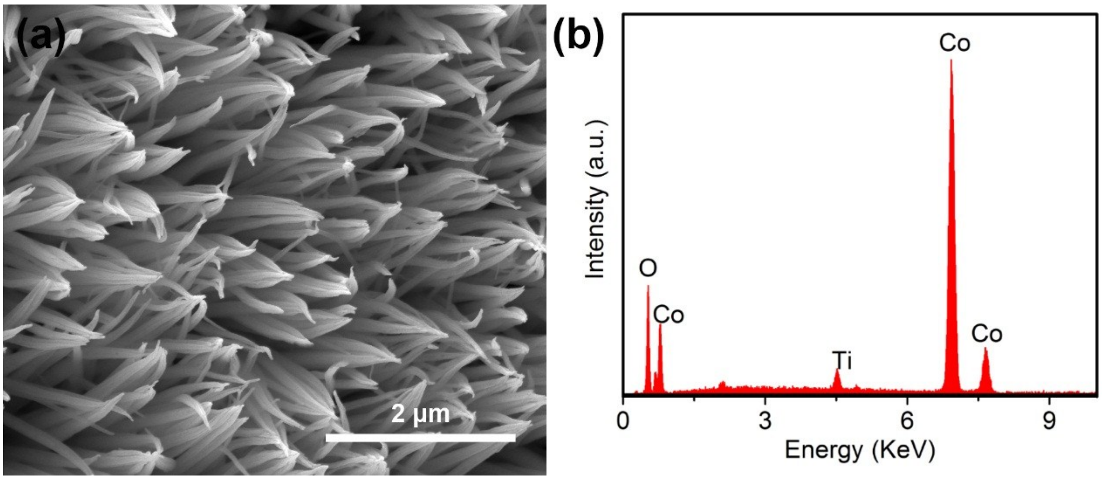

Figure S4. (a) SEM image of $Co_3O_4$. (b) EDS spectrum of $Co_3O_4$.

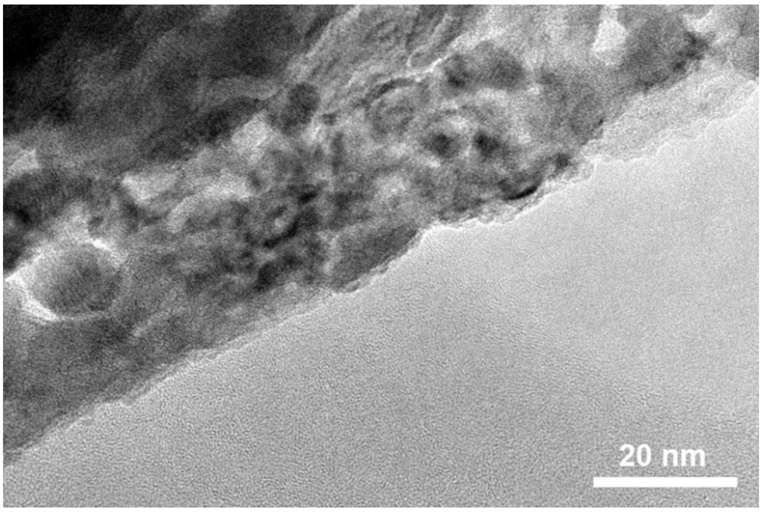

Figure S5. Enlarged TEM image of Pi-CoP.

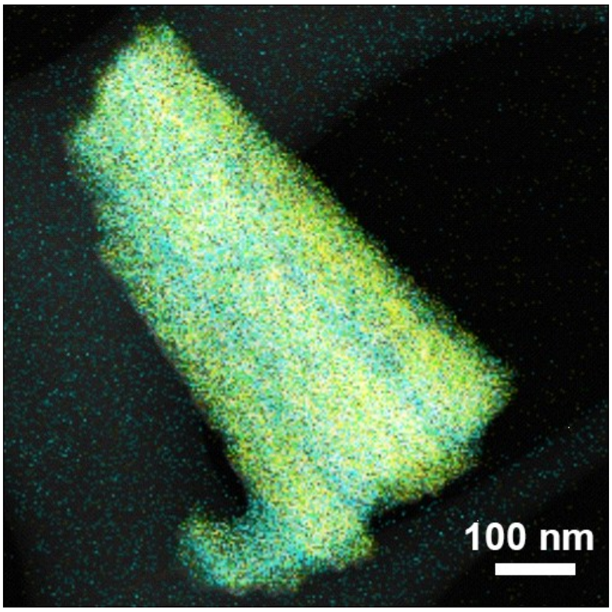

Figure S6. The overlay elemental mapping of Pi-CoP.

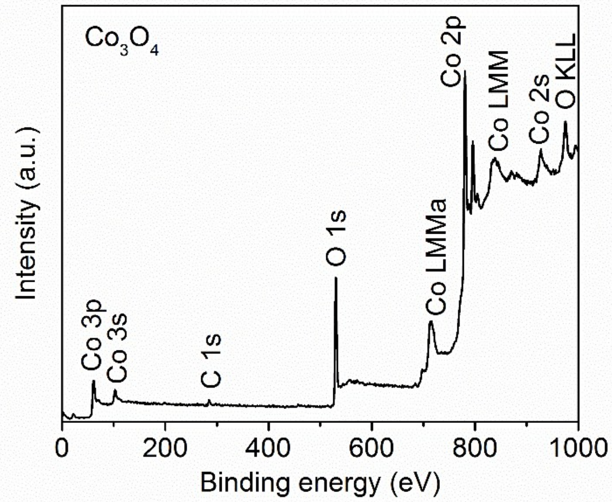

Figure S7. XPS survey spectrum of $Co_3O_4$.

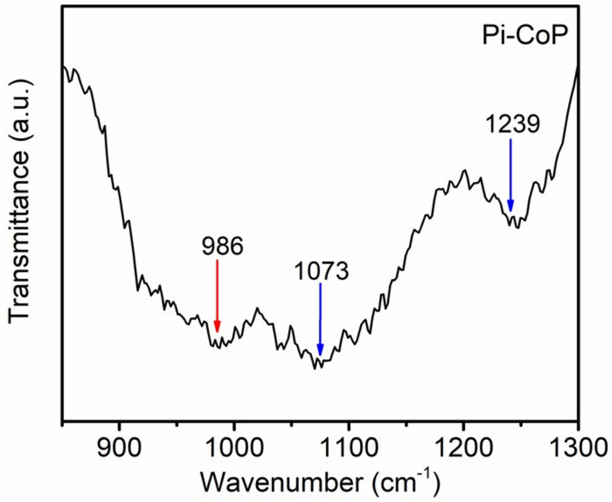

Figure S8. FTIR spectrum of Pi-CoP.

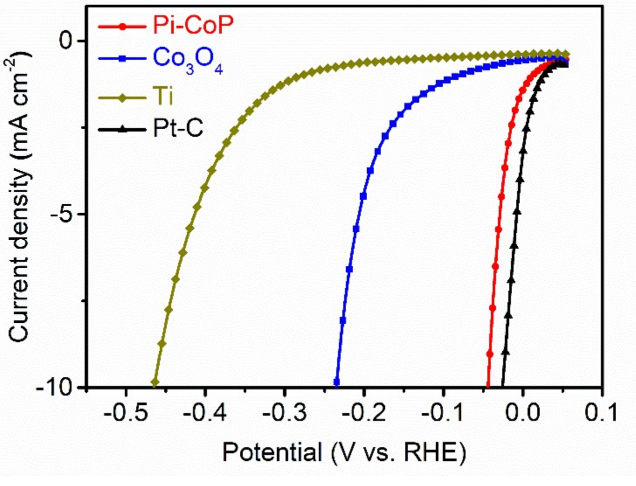

Figure S9. LSV curves of the samples to reach the current density of 10 mA cm$^{-2}$.

**Table S1.** HER performance comparison of previously reported transition metal phosphide-based electrocatalysts in alkaline solution.

| **Catalyst** | **Substrate** | **$\eta_{10}$ (mV)** | **$\eta_{100}$ (mV)** | **Tafel slop (mV dec$^{-1}$)** | **Reference** |
|---|---|---|---|---|---|
| Pi-CoP | Ti foil | 44 | 112 | 49 | This work |
| CoP | carbon cloth | 209 | 500 | 129 | 1 |
| FeP | carbon cloth | 218 | NA | 146 | 2 |
| W-$Ni_xP$ | nickel foam | 130 | NA | 98 | 3 |
| $Ni_2P$ | nickel foam | NA | >200 | 50 | 4 |
| NiP | nickel foam | 236 | 350 | 135 | 5 |
| $Ni_{0.51}Co_{0.49}P$ | nickel foam | 82 | 150 | 43 | 5 |
| $Ni_2P$ | Ni foil | 183 | NA | NA | 6 |
| FeCoP | nickel foam | 120 | NA | 76 | 7 |
| Fe-CoP | Ti foil | 78 | NA | 75 | 8 |
| Mn-$Ni_2P$ | nickel foam | NA | 200 | 135 | 9 |
| MoP/CNT | carbon fiber paper | 86 | 160 | 73 | 10 |
| CoP | carbon cloth | NA | 326 | 126.8 | 11 |
| CoP/$CoO_x$ | carbon cloth | NA | 146 | 42.8 | 11 |
| $CoP_2$ | carbon cloth | 72 | NA | 88 | 12 |
| V-CoP | carbon cloth | 71 | 140 | 67.6 | 13 |
| S-CoP | nickel foam | 109 | 185 | 79 | 14 |
| Al-$Ni_2P$ | Ti mesh | 129 | NA | 98 | 15 |
| $(Fe_{0.048}Ni_{0.952})_2P$ | nickel foam | 103 | 200 | 76.6 | 16 |

**$\eta_{10}$ :** Overpotential required at the current density of 10 mA cm$^{-2}$.

**$\eta_{100}$ :** Overpotential required at the current density of 100 mA cm$^{-2}$.

References

1. J. Tian, Q. Liu, A. M. Asiri and X. Sun, *J. Am. Chem. Soc.*, 2014, **136**, 7587-7590.
2. Y. Liang, Q. Liu, A. M. Asiri, X. Sun and Y. Luo, *ACS Catal.*, 2014, **4**, 4065-4069.
3. Z. Jin, P. Li, X. Huang, G. Zeng, Y. Jin, B. Zheng and D. Xiao, *J. Mater. Chem. A*, 2014, **2**, 18593-18599.
4. Y. Shi, Y. Xu, S. Zhuo, J. Zhang and B. Zhang, *ACS Appl. Mater. Interfaces*, 2015, **7**, 2376-2384.
5. J. Yu, Q. Li, Y. Li, C.-Y. Xu, L. Zhen, V. P. Dravid and J. Wu, *Adv. Funct. Mater.*, 2016, **26**, 7644-7651.
6. C. G. Read, J. F. Callejas, C. F. Holder and R. E. Schaak, *ACS Appl. Mater. Interfaces*, 2016, **8**, 12798-12803.
7. L. Zhou, M. Shao, J. Li, S. Jiang, M. Wei and X. Duan, *Nano Energy*, 2017, **41**, 583-590.
8. C. Tang, R. Zhang, W. Lu, L. He, X. Jiang, A. M. Asiri and X. Sun, *Adv. Mater.*, 2017, **29**, 1602441.
9. Y. Zhang, Y. Liu, M. Ma, X. Ren, Z. Liu, G. Du, A. M. Asiri and X. Sun, *Chem. Commun.*, 2017, **53**, 11048-11051.
10. X. Zhang, X. Yu, L. Zhang, F. Zhou, Y. Liang and R. Wang, *Adv. Funct. Mater.*, 2018, **28**, 1706523.
11. K. Xu, H. Cheng, H. Lv, J. Wang, L. Liu, S. Liu, X. Wu, W. Chu, C. Wu and Y. Xie, *Adv. Mater.*, 2018, **30**, 1703322.
12. Y. Zhou, Y. Yang, R. Wang, X. Wang, X. Zhang, L. Qiang, W. Wang, Q. Wang and Z. Hu, *J. Mater. Chem. A*, 2018, **6**, 19038-19046.
13. X. Xiao, L. Tao, M. Li, X. Lv, D. Huang, X. Jiang, H. Pan, M. Wang and Y. Shen, *Chem. Sci.*, 2018, **9**, 1970-1975.
14. M. A. R. Anjum, M. S. Okyay, M. Kim, M. H. Lee, N. Park and J. S. Lee, *Nano Energy*, 2018, **53**, 286-295.
15. H. Du, L. Xia, S. Zhu, F. Qu and F. Qu, *Chem. Commun.*, 2018, **54**, 2894-2897.
16. W. Zhang, Y. Zou, H. Liu, S. Chen, X. Wang, H. Zhang, X. She and D. Yang, *Nano Energy*, 2019, **56**, 813-822.